



Deciphering Transition Metal Diffusion in Anode Battery Materials: A Study on Nb Diffusion in $\text{Nb}_x\text{Ti}_{1-x}\text{O}_2$

Downloaded from: <https://research.chalmers.se>, 2025-09-25 12:11 UTC



Citation for the original published paper (version of record):

Forslund, O., Cavallo, C., Cedervall, J. et al (2025). Deciphering Transition Metal Diffusion in Anode Battery Materials: A Study on Nb Diffusion in $\text{Nb}_x\text{Ti}_{1-x}\text{O}_2$. Carbon Energy, 7(8). <http://dx.doi.org/10.1002/cey2.70017>

N.B. When citing this work, cite the original published paper.

RESEARCH ARTICLE OPEN ACCESS

Deciphering Transition Metal Diffusion in Anode Battery Materials: A Study on Nb Diffusion in $\text{Nb}_x\text{Ti}_{1-x}\text{O}_2$

Ola Kenji Forslund^{1,2,3}  | Carmen Cavallo⁴ | Johan Cedervall⁵  | Jun Sugiyama⁶ | Kazuki Ohishi⁶ | Akihiro Koda⁶ | Alessandro Latini⁷ | Aleksandar Matic¹ | Martin Månsson⁸ | Yasmine Sassa^{1,8}

¹Department of Physics, Chalmers University of Technology, Göteborg, Sweden | ²Department of Physics and Astronomy, Uppsala University, Uppsala, Sweden | ³Physik-Institut, Universität Zürich, Winterthurerstrasse 190, CH-8057, Zürich, Switzerland | ⁴Centre for Materials Science and Nanotechnology, Department of Chemistry, Oslo University, Oslo, Norway | ⁵Department of Chemistry Ångström Laboratory, Uppsala University, Uppsala, Sweden | ⁶Neutron Science and Technology Center, Comprehensive Research Organization for Science and Society (CROSS), Tokai, Ibaraki, Japan | ⁷Department of Chemistry, Sapienza University of Rome, Rome, Italy | ⁸Department of Applied Physics, KTH Royal Institute of Technology, Stockholm, Sweden

Correspondence: Ola Kenji Forslund (ola.forslund@physik.uzh.ch)

Received: 5 December 2024 | **Revised:** 2 February 2025 | **Accepted:** 9 February 2025

Funding: This study was supported by Vetenskapsrådet (2022-06217).

Keywords: batteries | diffusion | electrocatalysis | energy storage and conversion | muon spin relaxation | TiO_2 | transition metal

ABSTRACT

Demand for fast-charging lithium-ion batteries (LIBs) has escalated incredibly in the past few years. A conventional method to improve the performance is to chemically partly substitute the transition metal with another to increase its conductivity. In this study, we have chosen to investigate the lithium diffusion in doped anatase (TiO_2) anodes for high-rate LIBs. Substitutional doping of TiO_2 with the pentavalent Nb has previously been shown to increase the high-rate performances of this anode material dramatically. Despite the conventional belief, we explicitly show that Nb is mobile and diffusing at room temperature, and different diffusion mechanisms are discussed. Diffusing Nb in TiO_2 has staggering implications concerning most chemically substituted LIBs and their performance. While the only mobile ion is typically asserted to be Li, this study clearly shows that the transition metals are also diffusing, together with the Li. This implies that a method that can hinder the diffusion of transition metals will increase the performance of our current LIBs even further.

1 | Introduction

There is no question that the world demands better, safer, and more sustainable Li-ion battery (LIB) and Na-ion battery, which entails finding materials with high capacity and long lifetimes. One key parameter in electrode materials governing these attributes is the diffusion coefficient ($D_{\text{Li,Na}}$). Traditionally, these parameters are determined by electrochemical measurements and have successfully contributed to battery development during the last decades. However, the reactive surface area of a porous liquid electrode is nearly impossible to estimate accurately, and the determined $D_{\text{Li,Na}}$ usually has a large spread of several orders of magnitude. Moreover, other effects like

interfaces can also play a role besides bulk diffusivity, and it is sometimes impossible to separate different contributions.

To overcome these issues, Li/Na-nuclear magnetic resonance (NMR) has become a common probe to measure and successfully determine $D_{\text{Li,Na}}$ [1, 2]. However, an accurate determination of $D_{\text{Li,Na}}$ with NMR is challenging in case that the target compound contains *d*- or *f*-electron spins (typically a transition metal), as its fluctuation contributes to the spin-lattice relaxation rate ($1/T_1$) [3, 4]. Instead, the related technique, muon spin relaxation ($\mu^+\text{SR}$), has been adapted and developed for measurements on battery cathode materials [5]. It relies on implanting nearly 100% spin-polarised muons into the compound, which then acts as a

This is an open access article under the terms of the [Creative Commons Attribution](https://creativecommons.org/licenses/by/4.0/) License, which permits use, distribution and reproduction in any medium, provided the original work is properly cited.

© 2025 The Author(s). *Carbon Energy* published by Wenzhou University and John Wiley & Sons Australia, Ltd.

small magnetometer. The high gyromagnetic ratio of the muon allows it to detect even nuclear magnetic moments. Therefore, any fluctuations of nuclear moments can be detected as well, which includes fluctuations originating from diffusing ions with nuclear moments, for example, $I_{\text{Li}} = 3/2$ or $I_{\text{Na}} = 3/2$. Since the first experiment [5], which showed that the determined value of $D_{\text{Li,Na}}$ is comparable to that obtained using first principle calculations, detailed thermal diffusion has been clarified in many materials with $\mu^+\text{SR}$ [6–8].

Doping is a well-known strategy to enhance the electrochemical performance of electrode materials to mitigate undesirable structural transformations and thereby establish structural integrity during Li-ion transfers. For example, the incorporation of Mg and Al in the arch typical material LiCoO_2 showed the suppression of the undesired phase transition at voltages above 4.5 V [9]. Similar performance enhancement has been reported using almost any element in the periodic table including Nb, Ta, Ca, Mo, Te, and so forth [10]. However, there is a possibility that the substituted transition metal is not structurally stable as commonly believed. Since conventional electrochemical methods or other bulk techniques measure the whole sample, part of the results may be affected by a diffusing transition metal.

To confirm the outlined scenario, we have chosen $\text{Nb}_x\text{Ti}_{1-x}\text{O}_2$ and its lithiated phase as our target compounds to be investigated with $\mu^+\text{SR}$. From $\mu^+\text{SR}$ point of view, both Ti and O are practically invisible, given their low nuclear moments. Nb, on the other hand, has a very large nuclear moment with $I_{\text{Nb}} = 9/2$ and a natural abundance of 100% and contributes strongly to the measured signal. The presence of O in the compound entails a thermally stable muon as well [11]. Moreover, TiO_2 -based materials are considered to be structurally stable and thereby promising materials for electrodes. The value of the structure changes by about 4% during cycling, which asserts stability for charging rechargeable batteries. Here, substituting small amounts of pentavalent Nb ions at the nominal Ti sites [12] has shown to significantly improve the lifetime by reducing the decay of capacity and increasing the specific nominal capacity both at low and high current rates, which nominally makes these materials highly attractive for low- and high-rate capable fast rechargeable LIBs [13–17].

In this study, we evaluate the microscopic effects of Nb doping via $\mu^+\text{SR}$ on the compounds $\text{Li}_y\text{Nb}_x\text{Ti}_{1-x}\text{O}_2$ (for $x = 0.1$, $y = 1$; $x = 0.01$, $y = 1$; $x = 0.1$, $y = 0$ and $x = 0.01$, $y = 0$). As expected, we find evidence of fluctuating Li ions in the sample ($y = 0$). Remarkably, we observe strong internal magnetic field fluctuation in sample ($y = 0$) as well. These results suggest that Nb ions are not structurally stable as often assumed in the literature and show strong evidence of Nb diffusion, despite the robust structural stability of TiO_2 . This questions the legitimacy of doping as a performance booster in LIBs. Another way of looking at it is that a method to hinder the diffusion of transition metals will most likely increase the performance of current LIBs.

2 | Results

Figure 1 shows the $\mu^+\text{SR}$ time spectra for $\text{Li}_y\text{Nb}_x\text{Ti}_{1-x}\text{O}_2$ ($x = 0.1$, $y = 1$; $x = 0.01$, $y = 1$; $x = 0.1$, $y = 0$ and $x = 0.01$, $y = 0$) measured in zero field (ZF) and longitudinal field (LF) configurations at

$T = 60$ K. LF refers to the applied field direction, which is parallel to the initial muon spin polarisation. Here, the muon state may relax from one state to the other (which is called the spin-lattice relaxation rate), and this relaxation is caused when the nuclear dipole of a diffusing ion interacts with the muon. More details about ion diffusion with $\mu^+\text{SR}$ are presented elsewhere [18]. A Kubo-Toyabe (KT)-like depolarisation (originating from randomly distributed magnetic fields) is observed at this temperature, which develops into an exponential-like at higher temperatures. Since weak LF is able to decouple the time spectra, it is underlined that this KT depolarisation is manifested mainly from randomly oriented Nb and Li nuclear moments with $I_{\text{Nb}} = 9/2$ and $I_{\text{Li}} = 3/2$. Apart from the KT-like depolarisation, a small offset is also observed, attributed to the fraction of muons stopping inside the sample holder. However, a single Gaussian KT function is not able to fully reproduce the time spectra. A close inspection of the ZF curve reveals smaller anomalies. Therefore, the ZF + LF time spectra were fitted using a combination of two dynamic Gaussian KT (G^{DGKT} ; sample) and a non-relaxing asymmetry (sample holder) components:

$$A_0 P_{\text{ZFLF}}(t) = \sum_{i=1}^2 A_{\text{KT}i} G^{\text{DGKT}}(H_{\text{LF}}, \Delta_i, \nu_i, t) + A_{\text{BG}}, \quad (1)$$

where A_0 is the initial asymmetry determined by the instrument and $P_{\text{ZFLF}}(t)$ is the muon spin polarisation function in ZF and LF configurations ($H_{\text{LF}} = 0, 5$ and 10 G). A_{KT} , Δ and ν are the asymmetry, field distribution width and field fluctuation rate of the KT component, respectively, while A_{BG} is the asymmetry fraction originating from the sample holder. The origin behind the two separate KT is discussed below.

To obtain accurate fit parameters, the collected data were fitted in a so-called global fit procedure, where $A_{\text{KT}i}$ and A_{BG} were kept as temperature-independent parameters across the measured temperature range (60–410 K). This assertion is based on the assumption that the fraction of muons stopping on the Ti sample holder is temperature-independent and that the sample does not undergo a temperature-dependent structural transition. This is corroborated by our temperature-dependent X-ray diffraction (XRD) measurements which confirm the absence of any structural transition. Additionally, the applied magnetic LF can be considered small and the spin-spin correlations are most likely field-independent in this considered range. Thus, Δ and ν were kept common across the measured field configurations for the given temperature. Finally, $\nu_i = \nu$ was set for each temperature. Using the global fit procedure as described, $A_{\text{KT}1} = 0.0228(4)$ and $A_{\text{KT}2} = 0.1235(5)$ for $x = 0.1$, $y = 1$; $A_{\text{KT}1} = 0.0228(4)$ and $A_{\text{KT}2} = 0.1254(4)$ for $x = 0.01$, $y = 1$; $A_{\text{KT}1} = 0.0340(3)$ and $A_{\text{KT}2} = 0.1212(3)$ for $x = 0.1$, $y = 0$ and $A_{\text{KT}1} = 0.0398(4)$ and $A_{\text{KT}2} = 0.1096(4)$ for $x = 0.01$, $y = 0$ were obtained for the temperature-independent KT asymmetries.

The temperature-dependent parameters are shown in Figure 2. As the temperature increases, the value of Δ decreases monotonically, which is a result of an increase in internal magnetic field dynamics. This decrease saturates into a new high-temperature value and corresponds to a value in the motional narrowing limit (see below). A more direct measure of the dynamics is found in ν , which increases as the Δ decreases. The

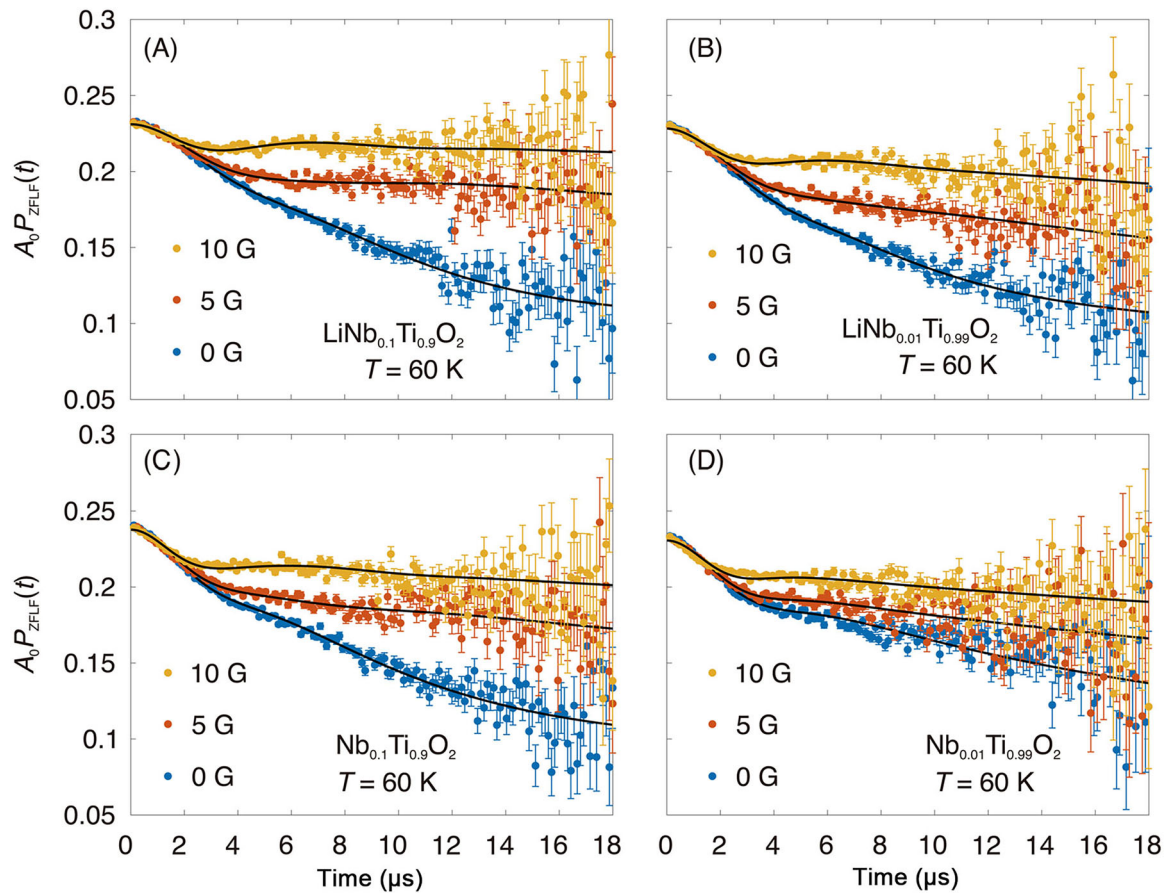


FIGURE 1 | ZF and LF time spectra collected at $T = 60$ K for (A) $\text{LiNb}_{0.1}\text{Ti}_{0.9}\text{O}_2$, (B) $\text{LiNb}_{0.01}\text{Ti}_{0.99}\text{O}_2$, (C) $\text{Nb}_{0.1}\text{Ti}_{0.9}\text{O}_2$ and (D) $\text{Nb}_{0.01}\text{Ti}_{0.99}\text{O}_2$. The solid lines represent the best fits using Equation 1.

increase in ν resembles an exponential increase and corresponds to an Arrhenius thermal activation process. Plotting the natural logarithm of ν as a function of the inverse temperature shows a linear dependence, clear evidence of an Arrhenius evolution (Figure 3). The derivative of the line corresponds to the activation energy, while the intersect is the prefactor of the Arrhenius equation (Table 1). It is noted that the dip in ν (Figure 2C,D) observed around 250–300 K corresponds to a point in which the internal field fluctuations increase above the sensitivity of the $\mu^+\text{SR}$ technique. These kinds of dips in ν have been observed in many battery materials [5, 18–20] using a similar experimental setup.

3 | Discussion

The absolute value of Δ is determined by the muon coupling to the nuclear bath, and the value in the static regime (at low temperature) can be reproduced by Van Vleck formalism for a given muon site. Therefore, we have performed density functional theory (DFT) calculations on TiO_2 (Supporting Information S1: Table 1) to predict the most probable muon sites. A self-consistent calculation using the pseudopotential-based plane-wave method, as implemented in Quantum Espresso [21], is performed to evaluate the charge landscape, in which the minimum is asserted to be the muon site. In this case, $(1/2, 1/2, 0)$ is predicted as the main muon site. Surprisingly, only one muon site is suggested by DFT. To verify if this site

belongs to the first (A_{KT1}) or the second signal (A_{KT2}), the expected Δ value is computed using the Van Vleck formalism and is shown in Figure 2. This calculation considers the static limit, that is, the low-temperature behaviour. These calculations confirm that the largest portion of the signal (A_{KT2}) originates from the predicted site: 84% for $x = 0.1$, $y = 1$; 85% for $x = 0.01$, $y = 1$; 78% for $x = 0.1$, $y = 0$ and 73% for $x = 0.01$, $y = 0$. Small mismatches between the calculated and measured Δ are common as the calculations do not consider minimal local distortions on the lattice induced by the muon. We confirm that better agreement can be achieved by introducing smaller distortions. However, a quantitative assessment of these distortions is challenging, and they are therefore not considered in the referenced values. That being said, the signal from the smaller portion (A_{KT1}) is not predicted within our method. We shall however point out that a hypothetical lattice NbO_2 yields $\Delta = 0.550136 \mu\text{s}^{-1}$ at the position $(1/2, 1/2, 0)$, which is consistent with the measured Δ_{KT1} . This would suggest that there is a small fraction of the sample that contains a cluster of Nb elements. Structurally, NbO_2 and TiO_2 are very similar, and such a cluster is most likely not observable with XRD.

This subtle distinction is possible to observe because of the high contrast between Nb and Ti nuclear moments, which is observable using a sensitive technique as $\mu^+\text{SR}$. Nonetheless, the main results and conclusion drawn (that Nb ions are diffusing at room temperature in both lithiated and non-lithiated samples) are not affected by this fact.

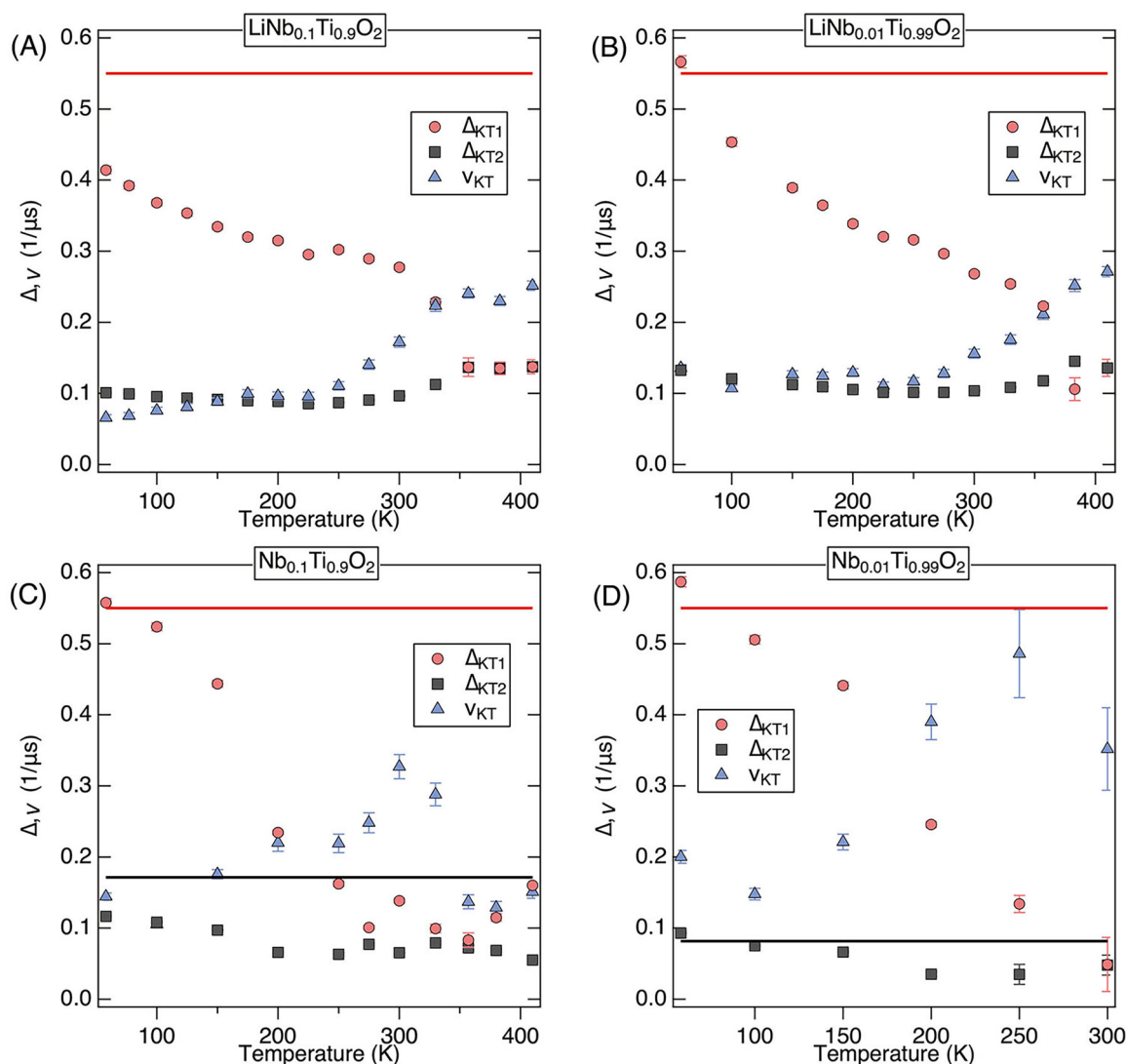


FIGURE 2 | Temperature-dependent Kubo-Toyabe (KT) fit parameters obtained from Equation 1 using the procedure described in the main text, for (A) $\text{LiNb}_{0.1}\text{Ti}_{0.9}\text{O}_2$, (B) $\text{LiNb}_{0.01}\text{Ti}_{0.99}\text{O}_2$, (C) $\text{Nb}_{0.1}\text{Ti}_{0.9}\text{O}_2$ and (D) $\text{Nb}_{0.01}\text{Ti}_{0.99}\text{O}_2$. The solid lines represent the expected Δ_{KT} values for $\text{Li}_y\text{Nb}_x\text{Ti}_{1-x}\text{O}_2$ structure (black) and the hypothetical NbO_2 structures (red) at (1/2,1/2,0) in the static limit (i.e., at low temperatures).

We propose that the decrease in Δ and an increase in ν is due to motional narrowing and diffusing Nb (and Li). Apart from the direct observation of an increase in ν , this assertion is confirmed once again by calculating the expected Δ but having the Nb (and Li) nuclear moments set to 0 (due to motional narrowing). In the motional narrowing limit, the affected nuclear moments will be fluctuating outside the sensitivity of μ^+ SR technique, which is approximately equivalent of having them not contributing to the spectra. In this approximation, $\Delta = 0.030 \mu\text{s}^{-1}$ is obtained. This value is close to the measured value of Δ_{KT1} and Δ_{KT2} at room temperature for the non-lithiated samples (Figure 2C,D). It is also noted that $\Delta_{\text{KT1}} \approx \Delta_{\text{KT2}}$ at room temperature. These are yet other strong evidence of Nb diffusion in title compounds. These assertions are consistent with reported μ^+ SR results on other battery compounds [5, 18, 19].

While the high-temperature data clearly show dynamic internal magnetic fields, there is a possibility that muon is the diffusing species. μ^+ SR has in the past successfully determined diffusing

species in various battery materials, mostly Li [5, 22], Na [19, 23] and even K [24] ions. Even though the stability of the muon has been a question, a recent combined study using both positive and negative μ^+ SR has clarified and confirmed the stability of muons in these compounds [20, 22]. Moreover, similar compounds such as $\text{Li}_4\text{Ti}_5\text{O}_{12}$ or LiTi_2O_4 [25] have shown the muon to be stable up to 400 K. Therefore, we can safely assert the muon to be static in our compounds as well. This implies that the dynamics observed at higher temperatures are originating from Nb and Li ion diffusion. This is also corroborated by the fact that the activation energies of the lithiated and nonlithiated samples are not the same (Table 1). If the muon was diffusing, one would expect the activation energies to be comparable. By similar arguments, fluctuations caused by any hypothetical impurities (e.g., H diffusion) are unlikely. This assertion is also corroborated by energy-dispersive X-ray spectroscopy (EDX) spectra of these samples presented in Cavallo et al. [12], which show the absence of such impurities. Instead, the average activation energies for Nb ≈ 14.85 meV and Li ≈ 53.1 meV are obtained. In fact, Li-NMR data on LiTiO_2 [26] show clear motional narrowing effects at

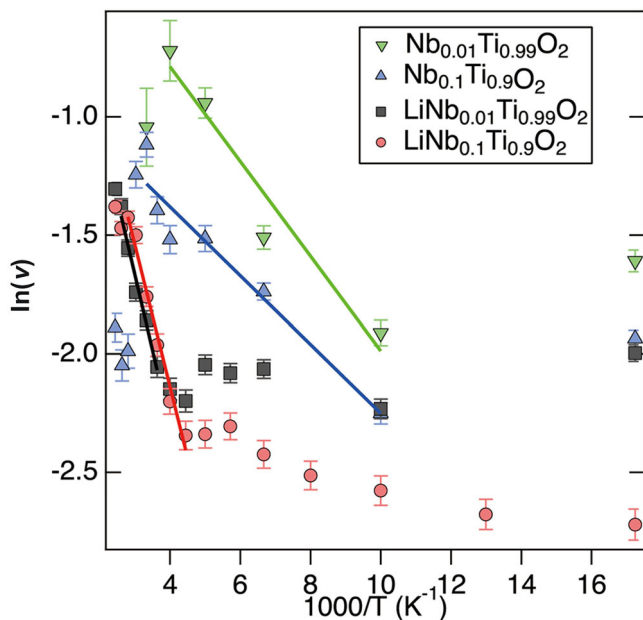


FIGURE 3 | The natural logarithm of the field fluctuation rate presented in Figure 2, plotted against the inverse temperature. The solid lines represent the best fits using the line equation.

TABLE 1 | The obtained Arrhenius parameters ($\nu = Ae^{-Ea/kBT}$) from the line fits presented in Figure 3.

Sample	Ea (meV)	$\ln(A)$
Li _{0.9} Nb _{0.1} TiO ₂	51.6 (3.6)	0.26 (15)
Li _{0.99} Nb _{0.01} TiO ₂	54.6 (4.4)	0.23 (16)
Nb _{0.1} TiO ₂	12.5 (1.7)	−0.80 (12)
Nb _{0.01} TiO ₂	17.2 (2.9)	0.01 (23)

temperatures comparable to our results. This is a clear indication that the muon is static in TiO₂ and our assertions are correct, namely that Li and Nb are diffusing at higher temperatures (including room temperature). Nevertheless, we hope our findings can be directly verified via future μ -SR or neutron scattering.

With the diffusing species clarified, we wish to discuss what consequences a diffusing Nb has in terms of battery point of view. While it is not possible to determine the diffusing mechanism of Nb directly from the data, we can make an educated guess based on the observed behaviours and the crystal structure. We shall first note that even in the lithiated sample, Nb is most likely diffusing already before the Li diffusion starts. This is seen in Figure 3, in which a slope is observed at a lower temperature of $x=0.1$, $y=1$. A similar slope is not observed in $x=0.01$, $y=1$ because of the low fraction of Nb compared with Li. The activation energy and the absolute value of ν , which is directly proportional to D_{Li} , are comparable between the two samples of $y=0$. This suggests that the diffusivity in itself is not hindered by the presence of diffusing Nb. Moreover, an Arrhenius process clearly describes diffusion activation in the compounds ($y=1$); the $y=0$ activation does not seem to be as well described by this model (Figure 3). This in turn implies that the diffusing

mechanism/path of Nb is different from that of Li. It is well known that Li diffuses thermally through interstitial or vacancy mechanism [27]. The conclusion is therefore that Nb diffusion is not interstitial/vacancy (as such diffusion would physically hinder the diffusion [28]). Instead, the Nb is likely to directly or indirectly frequently exchange positions with Ti.

The Nb atoms occupy the same crystallographic position as Ti. Chemically, breaking an O–Nb bond by leaving a neighboring Nb site unoccupied is unfavorable and leads to lattice reconstruction. Additionally, since Nb is larger than Ti, a transition to an interstitial position is unlikely. Instead, Nb diffusion must proceed without disrupting Li diffusion while preserving the structural integrity. One mechanism that satisfies these conditions involves Nb swapping positions with Ti, as both occupy the same Wyckoff sites. This process can occur without hindering Li thermal diffusion in these compounds. Furthermore, this is consistent with the observation that Nb diffusion occurs without any structural phase transition. Detailed calculations are required to validate the exchange pathways and mechanism, which will be addressed in future work.

Compared to other high-rate materials such as Li₄Ti₅O₁₂ and Nb-doped LiMn₂O₄ [29, 30], our findings provide a new insight into transition metal dynamics, setting a precedent by revealing that Nb ions exhibit mobility even at room temperature. Recent reviews have highlighted the advantages of TiO₂ as an anode material due to its low volume fluctuations (<4%), safety and structural durability [31]. However, these studies have focused on lithium-ion intercalation and did not consider the possibility of dopant mobility. Emerging techniques, such as machine learning-based predictions of doped TiO₂ performance, have emphasized the importance of dopants in enhancing electronic and electrochemical properties. Yet, the potential mobility of the doped transition metals themselves was not addressed [32]. In addition, studies on layered structure 2D MXene/TiO₂ composites have demonstrated excellent electronic conductivity and high structural stability [33], but transition metal mobility within these systems remains unexplored.

Our study demonstrates, for the first time, the mobility of Nb ions in doped TiO₂ anodes for high-rate LIBs. This discovery fundamentally challenges the conventional belief that transition metals remain immobile in systems where structural stability is crucial to improving performance and increasing D_{Li} . Since the most common diffusion mechanism for Li in LIBs is interstitial or vacancy diffusion, we suggest that hindering Nb diffusion in LiNb_xTi_{1-x}O₂ will improve the performance even further. In fact, this assertion is consistent with the observed behaviour of Mn dissolution in LiMn₂O₄ due to corrosion [34]. On the other hand, previous electrochemical studies on Nb-doped TiO₂ suggest increased cycle lifetime [12, 35], attributed to reduction in strain during the Li insertion, and it may be that this reduction in strain is assisted by Nb diffusion. As a matter of fact, recent phonon studies have suggested a mechanism in which phonons assist the diffusion of the alkali ions [36]. It would be interesting to continue similar study on the presented compound considering the mobile Nb. Finally, we wish to state that while we have asserted Li and Nb to be mobile in the title compounds, we cannot assert the situation for Ti given that its signal is undetectable in this case from μ^+ SR point of view.

4 | Conclusions

While chemical substitution is a common method to enhance the performance of various battery materials, this study shows that even transition metals are mobile, diffusing at room temperature. We provide strong, direct and microscopic evidence of Nb diffusion in $\text{Li}_y\text{Nb}_x\text{Ti}_{1-x}\text{O}_2$. Although alkali ions are typically considered the primary diffusing species in transition-metal-based battery materials, our results suggest that this assumption does not always hold. Moreover, diffusing transition metals may affect the measurements presented in the literature and inevitably the battery lifetime and performance. We hope this study encourages the wider use of microscopic probes to measure battery materials to ensure their microscopic stability in regard to the transition metals. Finally, we wish to note that $\mu^+\text{SR}$ has been used to detect the diffusion of Li, Na and even K ions but this is the first instance of Nb diffusion.

5 | Lead Contacts

Inquiries regarding the data and sample related to this paper can be directed to Dr. Ola K. Forslund (ola.forslund@physik.uzh.ch) or Dr. Carmen Cavallo (cc@cenate.com).

6 | Experimental Setup

Titanium(IV) isopropoxide (TIP) (97+%), ammonium hydroxide solution (30%–33%), potassium chloride (KCl) (99.99%, trace metal basis), 1-hexadecyl amine (HDA) (technical, 90%) and niobium(V) ethoxide (99.95% trace metals basis) were purchased from Sigma Aldrich and used as received. The mesoporous anatase beads doped with Nb^{5+} were prepared according to the previous methodology [12]. Sample characterisations are presented in Supporting Information File S1 and in our previous work [12].

Temperature-dependent XRD patterns were recorded using a Bruker D8 diffractometer equipped with a LynxEye position-sensitive detector (PSD, 4° openings) using $\text{CuK}\alpha 1$ radiation ($\lambda = 1.5406 \text{ \AA}$). The measurements were performed between 100 and 300 K (2θ range of 10°–100°). All patterns could be fully refined using the anatase structure (space group $I4_1amd$) using one Ti(Nb) position (0, 1/4, 3/8) and one O position (0, 1/4, ~0.165). The difference in unit cell parameters on cooling from 300 to 100 K for each sample was minuscule, less than 1%. Additionally, no extra features appeared during cooling, indicating phase transitions in the samples. More details are presented in Supporting Information File S1.

The $\mu^+\text{SR}$ measurements were performed in double pulse mode at the surface muon beamline S1 in J-PARC (Japan). About 700–900 mg of samples were each prepared inside a He glove box, mounted into a Ti-made sample cell and sealed with a Ti-window (50 μm thick) and Au O-ring. A standard ^4He cryo-furnace was used to reach temperatures from 60 up to 410 K. Finally, the software *musrfit* [37] was used to analyse the muon data. Detailed descriptions of $\mu^+\text{SR}$ are found elsewhere [38, 39].

Acknowledgments

The $\mu^+\text{SR}$ experiment was conducted under proposal number 2020B0264. We acknowledge the support of the S1 beamline staff. O.K.F. and Y.S. are supported by the Swedish Research Council (VR) through a Starting Grant (Dnr. 2017-05078) and M.M. through a Marie Skłodowska-Curie Action and the Swedish Research Council - VR (Dnr. 2014-6426 and 2016-06955) as well as the Carl Tryggers Foundation for Scientific Research (CTS-18:272). O.K.F. is supported by the Swedish Research Council (VR) through Grant 2022-06217, the Foundation Blanceflor fellow scholarships for 2023 and 2024, and the Ruth and Nils-Erik Stenbäck Foundation. Y.S. acknowledges the funding from the Area of Advance-Material Sciences from Chalmers University of Technology. J.C. is supported by ÅForsk via the grant 22-378. J.S. was supported by the Japan Society for the Promotion Science (JSPS) KAKENHI Grant Nos. JP20K1149, JP23H01840 and JP24H00042. The authors acknowledge Dr. Muhammad E. Abdelhamid for helping with the synthesis of the prelithiated materials.

Conflicts of Interest

The authors declare no conflicts of interest.

Data Availability Statement

The data supporting the findings of this study can be shared upon request to the lead contacts.

References

1. C. P. Grey and N. Dupré, “NMR Studies of Cathode Materials for Lithium-Ion Rechargeable Batteries,” *Chemical Reviews* 104, no. 10 (2004): 4493–4512.
2. P. Heitjans, S. Indris, and M. Wilkening, “Solid-State Diffusion and NMR,” *Diffusion Fundamentals* 2 (2005): 1–20.
3. K. Nakamura, H. Ohno, K. Okamura, Y. Michihiro, I. Nakabayashi, and T. Kanashiro, “On the Diffusion of Li^+ Defects in LiCoO_2 and LiNiO_2 ,” *Solid State Ionics* 135, no. 1 (2000): 143–147.
4. A. Van der Ven, “Lithium Diffusion in Layered Li_xCoO_2 ,” *Electrochemical and Solid-State Letters* 3, no. 7 (May 1999): 301.
5. J. Sugiyama, K. Mukai, Y. Ikeda, H. Nozaki, M. Månsson, and I. Watanabe, “Li Diffusion in Li_xCoO_2 Probed by Muon-Spin Spectroscopy,” *Physical Review Letters* 103 (September 2009): 147601.
6. J. Sugiyama, H. Nozaki, M. Harada, et al., “Magnetic and Diffusive Nature of LiFePO_4 Investigated by Muon Spin Rotation and Relaxation,” *Physical Review B* 84 (2011): 054430.
7. J. Sugiyama, I. Umegaki, M. Matsumoto, et al., “Desorption Reaction in MgH_2 Studied With In Situ $\mu^+\text{SR}$,” *Sustainable Energy & Fuels* 3 (2019): 956–964.
8. I. McClelland, B. Johnston, P. J. Baker, M. Amores, E. J. Cussen, and S. A. Corr, “Muon Spectroscopy for Investigating Diffusion in Energy Storage Materials,” *Annual Review of Materials Research* 50, no. 1 (2020): 371–393.
9. J. N. Zhang, Q. Li, C. Ouyang, et al., “Trace Doping of Multiple Elements Enables Stable Battery Cycling of LiCoO_2 at 4.6 V,” *Nature Energy* 4, no. 7 (2019): 594–603.
10. H. Qian, H. Ren, Y. Zhang, et al., “Surface Doping vs. Bulk Doping of Cathode Materials for Lithium-Ion Batteries: A Review,” *Electrochemical Energy Reviews* 5, no. 4 (2022): 2.
11. S. B. Sulaiman, N. Sahoo, S. Srinivas, et al., “Theory of Location and Associated Hyperfine Properties of the Positive Muon in La_2CuO_4 ,” *Hyperfine Interactions* 84, no. 1 (1994): 87–103.
12. C. Cavallo, G. Calcagno, R. P. de Carvalho, et al., “Effect of the Niobium Doping Concentration on the Charge Storage Mechanism of

- Mesoporous Anatase Beads as an Anode for High-Rate Li-Ion Batteries,” *ACS Applied Energy Materials* 4, no. 1 (2021): 215–225.
13. L. R. Sheppard, T. Bak, and J. Nowotny, “Electrical Properties of Niobium-Doped Titanium Dioxide. 1. Defect Disorder,” *Journal of Physical Chemistry B* 110, no. 45 (2006): 22447–22454.
 14. K. Yang, Y. Dai, B. Huang, and Y. P. Feng, “First-Principles GGA+U Study of the Different Conducting Properties in Pentavalent-Ion-Doped Anatase and Rutile TiO₂,” *Journal of Physics D: Applied Physics* 47, no. 27 (2014): 275101.
 15. M. Matsubara, R. Saniz, B. Partoens, and D. Lamoen, “Doping Anatase TiO₂ With Group V-b and VI-b Transition Metal Atoms: A Hybrid Functional First-Principles Study,” *Physical Chemistry Chemical Physics* 19 (2017): 1945–1952.
 16. A. Tomaszewska, Z. Chu, X. Feng, et al., “Lithium-Ion Battery Fast Charging: A Review,” *eTransportation* 1 (2019): 100011.
 17. E. R. Logan and J. R. Dahn, “Electrolyte Design for Fast-Charging Li-Ion Batteries,” *Trends in Chemistry* 2, no. 4 (2020): 354–366.
 18. O. K. Forslund, R. Toft-Petersen, V. David, et al., Li-Ion Diffusion in Single Crystal LiFePO₄ Measured by Muon Spin Spectroscopy, arXiv:2111.11941 (2021), <https://arxiv.org/abs/2111.11941>.
 19. O. K. Forslund, H. Ohta, K. Kamazawa, et al., “Revisiting the *a*-Type Antiferromagnet NaNiO₂ With Muon Spin Rotation Measurements and Density Functional Theory Calculations,” *Physical Review B* 102 (November 2020): 184412.
 20. J. Sugiyama, O. K. Forslund, E. Nocerino, et al., “Lithium Diffusion in LiMnPO₄ Detected With μ^{\pm} SR,” *Physical Review Research* 2 (July 2020): 033161.
 21. P. Giannozzi, O. Andreussi, T. Brumme, et al., “Advanced Capabilities for Materials Modelling With Quantum ESPRESSO,” *Journal of Physics: Condensed Matter* 29, no. 46 (2017): 465901.
 22. J. Sugiyama, K. Ohishi, O. K. Forslund, et al., “How Li Diffusion in Spinel Li[Ni_{1/2}Mn_{3/2}]O₄ is Seen With μ^{\pm} SR,” *Zeitschrift für Physikalische Chemie* 236, no. 6–8 (2022): 799–816.
 23. M. Månsson and J. Sugiyama, “Muon-Spin Relaxation Study on Li- and Na-Diffusion in Solids,” *Physica Scripta* 88, no. 6 (2013): 068509.
 24. N. Matsubara, E. Nocerino, O. K. Forslund, et al., “Magnetism and Ion Diffusion in Honeycomb Layered Oxide Ni₂TeO₆,” *Scientific Reports* 10, no. 1 (2020): 18305.
 25. J. Sugiyama, H. Nozaki, I. Umegaki, et al., “Li-Ion Diffusion in Li₄-Ti₅O₁₂ and LiTi₂O₄ Battery Materials Detected by Muon Spin Spectroscopy,” *Physical Review B* 92 (2015): 014417.
 26. M. Wagemaker. *Structure and Dynamics of Lithium in Anatase TiO₂* (Delft University Press, 2003), 142.
 27. J. B. Richard and G. J. Dienes, *An Introduction To Solid State Diffusion* (Elsevier, 2012).
 28. E. Nocerino, O. K. Forslund, H. Sakurai, et al., “Na-Ion Dynamics in the Solid Solution Na_xCa_{1-x}Cr₂O₄ Studied by Muon Spin Rotation and Neutron Diffraction,” *Sustainable Energy & Fuels* 8 (2024): 1424–1437.
 29. L. Leng, J. Li, X. Zeng, et al., “Spinel LiMn₂O₄ Nanoparticles Grown in Situ on Nitrogen-Doped Reduced Graphene Oxide as an Efficient Cathode for a LiO₂/Li-Ion Twin Battery,” *ACS Sustainable Chemistry & Engineering* 7, no. 1 (2019): 430–439.
 30. M. M. Thackeray and K. Amine, “Li₄Ti₅O₁₂ Spinel Anodes,” *Nature Energy* 6, no. 6 (2021): 683.
 31. S. Paul, M. A. Rahman, S. B. Sharif, J. H. Kim, S. Siddiqui, and M. Hossain, “TiO₂ as an Anode of High-Performance Lithium-Ion Batteries: A Comprehensive Review Towards Practical Application,” *Nanomaterials* 12, no. 12 (2022): 2034.
 32. M. Jiang, Y. Zhang, Z. Yang, et al., “A Data-Driven Interpretable Method to Predict Capacities of Metal Ion Doped TiO₂ Anode Materials for Lithiumion Batteries Using Machine Learning Classifiers,” *Inorganic Chemistry Frontiers* 10 (2023): 6646–6654.
 33. Y. Jia, J. Liu, and L. Shang, “Layered Structure 2D MXene/TiO₂ Composites as High-Performance Anodes for Lithium-Ion Batteries,” *Ionics* 29, no. 2 (2023): 531–537.
 34. G. Zhou, X. Sun, Q. H. Li, et al., “Mn Ion Dissolution Mechanism for Lithium-Ion Battery With LiMn₂O₄ Cathode: In Situ Ultraviolet-Visible Spectroscopy and Ab Initio Molecular Dynamics Simulations,” *Journal of Physical Chemistry Letters* 11, no. 8 (2020): 3051–3057.
 35. S. Lindberg, C. Cavallo, G. Calcagno, A. M. Navarro-Suárez, P. Johansson, and A. Matic, “Electrochemical Behaviour of Nb-Doped Anatase TiO₂ Microbeads in an Ionic Liquid Electrolyte,” *Batteries & Supercaps* 3, no. 11 (2020): 1233–1238.
 36. P. Benedek, N. Yazdani, H. Chen, et al., “Surface Phonons of Lithium Ion Battery Active Materials,” *Sustainable Energy & Fuels* 3 (2019): 508–513.
 37. A. Suter and B. M. Wojek, “Musfit: A Free Platform Independent Framework for μ SR Data Analysis,” *Physics Procedia* 30 (2012): 69–73.
 38. A. Yaouanc and P. D. D. Reotier, *Muon Spin Rotation, Relaxation, and Resonance: Applications to Condensed Matter*, Number 147 (Oxford University Press, 2011).
 39. O. K. Forslund, “1D to 3D Magnetism in Quantum Materials: A study by Muons, Neutrons & X-Rays” (PhD diss., Kungliga Tekniska Högskolan, 2021).

Supporting Information

Additional supporting information can be found online in the Supporting Information section.